Mathematics

http://www.aimspress.com/journal/Math

AIMS Mathematics, 7(2): 1775–1790.
DOI: 10.3934/math.2022102
Received: 11 June 2021
Accepted: 04 October 2021
Published: 02 November 2021

Research article

An inertial parallel algorithm for a finite family of G-nonexpansive mappings applied to signal recovery

Nipa Jun-on[1], **Raweerote Suparatulatorn**[2,*], **Mohamed Gamal**[3] **and Watcharaporn Cholamjiak**[4,*]

[1] Faculty of Sciences, Lampang Rajabhat University, Lampang 52100, Thailand
[2] Department of Mathematics, Faculty of Science, Chiang Mai University, Chiang Mai 50200, Thailand
[3] Department of Mathematics, Faculty of Science, South Valley University, Qena 83523, Egypt
[4] School of Science, University of Phayao, Phayao 56000, Thailand

* **Correspondence:** Email: raweerote.s@gmail.com, c-wchp007@hotmail.com.

Abstract: This study investigates the weak convergence of the sequences generated by the inertial technique combining the parallel monotone hybrid method for finding a common fixed point of a finite family of G-nonexpansive mappings under suitable conditions in Hilbert spaces endowed with graphs. Some numerical examples are also presented, providing applications to signal recovery under situations without knowing the type of noises. Besides, numerical experiments of the proposed algorithms, defined by different types of blurred matrices and noises on the algorithm, are able to show the efficiency and the implementation for LASSO problem in signal recovery.

Keywords: weak convergence; parallel algorithm; G-nonexpansive; inertial extrapolation; numerical discussion
Mathematics Subject Classification: 47H04, 47H10

1. Introduction

Let $\boldsymbol{H}$ be a real Hilbert space with inner product $\langle ., . \rangle$ and the induced norm $\|.\|$. Let C be a nonempty subset of $\boldsymbol{H}$, and let $\triangle$ denotes the diagonal of the cartesian product $C \times C$, i.e., $\triangle = \{(x, x) : x \in C\}$. For a directed graph G such that the set $V(G)$ of its vertices coincides with C and the set $E(G)$ of its edges contains all loops, i.e., $E(G) \supseteq \triangle$. We assume G has no parallel edge. So we can identify the graph G with the pair $(V(G), E(G))$. A mapping $T : C \to C$ is said to be G-contraction if T satisfies the conditions:

($G1$) T is edge-preserving, i.e.,

$$(x, y) \in E(G) \quad \Rightarrow \quad (Tx, Ty) \in E(G).$$

($G2$) T decreases weights of edges of G, i.e., there exists $\delta \in (0, 1)$ such that

$$(x, y) \in E(G) \quad \Rightarrow \quad \|Tx - Ty\| \leq \delta \|x - y\|.$$

A mapping $T : C \to C$ is said to be G-nonexpansive if T satisfies the condition ($G1$) and
($G3$) T non-increases weights of edges of G, i.e.,

$$(x, y) \in E(G) \quad \Rightarrow \quad \|Tx - Ty\| \leq \|x - y\|.$$

The set of a fixed point of T is denoted by $F(T)$, that is, $F(T) = \{z \in \boldsymbol{H} : Tz = z\}$.

In 2008, by using the concepts in fixed point theory and graph theory, Jachymski [17] proved some generalizations of Banach's contraction principle in complete metric spaces endowed with a graph. Then in 2012, Aleomraninejed et al. [2] introduced some iterative G-contraction schemes with G-nonexpansive mappings in Banach spaces endowed with a graph. Recently, Alfuraidan and Khamsi [3] studied the existence of fixed points and proved a convergence result of monotone nonexpansive mapping on a Banach space endowed with a directed graph. Later on, many authors have discussed the Browder convergence theorem that deliberated the weak and strong convergence of some methods for G-nonexpansive mapping in a Hilbert space with a directed graph (see for example [2–4, 13, 32, 33]).

Motivated by the work of [1, 23], Suparatulatorn et al. [28] scrutinized the following modified S-iteration scheme:

$$\begin{cases} x_0 \in C, \\ y_n = (1 - \sigma_n)x_n + \sigma_n T_1 x_n, \\ x_{n+1} = (1 - \delta_n)T_1 x_n + (1 - \delta_n)T_2 y_n, \; n \geq 0, \end{cases}$$

where $\{\delta_n\}$ and $\{\sigma_n\}$ are sequences in $(0, 1)$ and $T_1, T_2 : C \to C$ are G-nonexpansive mappings. Additionally, they proved weak and strong convergence in order to approximate common fixed points of two G-nonexpansive mappings in a uniformly convex Banach space $\boldsymbol{X}$ endowed with a graph under this iteration.

Otherwise, speeding up the convergence of the algorithm has been interesting by many mathematicians, one of that is inertial extrapolation, which was initially proposed by Polyak [22] as an acceleration process. This algorithm was used to solve various convex minimization problems based on the heavy ball method of the two-order time dynamical system. Inertial type methods involve two iterative steps that the second step is obtained from the previous two iterates. These methods are committed to being considered as an efficient technique to deal with various iterative algorithms, particularly with the projection-based algorithms, see in [5, 8, 9, 21, 30, 31, 34].

Very recently, Suantai et al. [27] used the idea of Anh and Hieu [6, 7] to present the convergence of the algorithm using the shrinking projection method with the parallel monotone hybrid method for approximating common fixed points of a finite family of G-nonexpansive mappings. The application of the algorithm has been provided to signal recovery in a situation without knowing the type of noise.

This algorithm is defined in a real Hilbert space as follows:

$$\begin{cases} x_1 \in C,\ C_0 = C, \\ v_n^i = \alpha_n^i x_n + (1-\alpha_n^i) T_i x_n,\ i = 1,2,...,N, \\ i_n = \operatorname{argmax}\{\|v_n^i - x_n\| : i = 1,2,...,N\}, \bar{v}_n := v_n^{i_n}, \\ C_{n+1} = \{v \in C_n : \|v - \bar{v}_n\| \le \|v - x_n\|\}, \\ x_{n+1} = P_{C_{n+1}} x_1,\ n \ge 1, \end{cases} \tag{1.1}$$

where $\{\alpha_n^i\}$ is a sequence in $[0,1]$ such that $\liminf\limits_{n\to\infty} \alpha_n^i(1-\alpha_n^i) > 0$ for all $i = 1,2,...,N$. $\bar{v}_n$ is chosen by the optimization all v_n^i with x_n. After that, the closed convex set C_{n+1} was constructed by $\bar{v}_n$. Finally, the next approximation x_{n+1} is defined as the projection of x_1 on to C_{n+1}. More recently, Cholamjiak et al. [11] proposed an inertial forward-backward splitting algorithm for finding the solution of common variational inclusion problems based on the inertial technique and parallel monotone hybrid methods. They proved strong convergence results under some suitable conditions in Hilbert spaces. Here in this paper, the algorithm was very useful in image restoration. For given initial points $x_0, x_1 \in C_1 = \boldsymbol{H}$, let the sequences $\{x_n\}, \{y_n\}$ be generated by

$$\begin{cases} y_n = x_n + \theta_n(x_n - x_{n-1}), \\ z_n^i = (1-\alpha_n^i) y_n + \alpha_n^i J_{r_n}^B (I - r_n A_i) y_n,\ \ i = 1,2,...,N, \\ i = \operatorname{argmax}\{\|z_n^i - x_n\| :\ i = 1,2,...,N\},\ \bar{z}_n = z_n^i, \\ C_{n+1} = \{v \in C_n :\ \|\bar{z}_n - v\|^2 \le \|x_n - v\|^2 + \theta_n^2 \|x_n - x_{n-1}\|^2 - 2\theta_n \langle x_n - v, x_{n-1} - x_n\rangle\}, \\ x_{n+1} = P_{C_{n+1}} x_1,\ n \ge 1, \end{cases} \tag{1.2}$$

where $A_i : \boldsymbol{H} \to \boldsymbol{H}$ and $B : \boldsymbol{H} \to 2^{\boldsymbol{H}}$ are monotone operator with $J_{r_n}^B = (I + r_n B)^{-1}$, $\{r_n\} \subset (0, 2\alpha)$, $\{\theta_n\} \subset [0, \theta]$ for some $\theta \in [0,1]$ and $\{\alpha_n^i\}$ is a sequence in $[0,1]$ for all $i = 1,2,...,N$. It has been notable that if $\{r_n\} \subset (0, 2\alpha)$ where α is a constant of inverse strongly monotone operator A, then the mapping $J_{r_n}^B(I - r_n A)$ is nonexpansive. Later on, there have been some results involving the parallel method for solving the fixed point problem (see [10, 12, 14–16, 29]). One of the algorithms for solving common fixed point problems of the concerned nonexpansive operators is distributed inexact averaged operator algorithm (DIO) which is introduced by Li and Feng [20]. The DIO algorithm is proposed as follow:

$$x_{i,n+1} = \hat{x}_{i,n} + \alpha_{i,n}(F_i(\hat{x}_{i,n}) + \epsilon_{i,n} - \hat{x}_{i,n}),$$

for all $i = 1,2,...,N$, where $\hat{x}_{i,n}$ is defined by $\hat{x}_{i,n} := \sum_{j=1}^N a_{ij,n} x_{j,n}$, $\epsilon_{i,n} \in \boldsymbol{H}$ is an error for $F_i(\hat{x}_{i,n})$ and $F_i : \boldsymbol{H} \to \boldsymbol{H}$ is a nonexpansive for all $i = 1,2,...,N$. Under the conditions $\sum_{j=1}^N a_{ij,n} = 1$ for all $i = 1,2,...,N$ with $a_{ij,n} \ge a > 0$ and $\alpha_{i,n} \in [\alpha, 1-\alpha]$ for some constant $\alpha \in (0, \frac{1}{2})$, weak convergence theorem was proved in Hilbert spaces.

In this paper, a parallel algorithm for finding a common fixed point of a finite family of G-nonexpansive mappings using inertial technique is proposed. Also, the weak convergence theorem is proved by assuming some control conditions in a Hilbert space endowed with graphs. Furthermore, examples and numerical results for supporting the main results of this study are provided, and the convergence rate of the iterative methods from this study is compared. Moreover, the proposed algorithm is applied to solve signal recovery problems. Finally, the last section presents the numerical results.

2. Preliminaries

In this section, some known definitions and lemmas which will be used in the later sections are stated.

Lemma 2.1. [5] *Let* $\{\psi_n\}$, $\{\delta_n\}$ *and* $\{\alpha_n\}$ *be the sequences in* $[0,+\infty)$ *such that* $\psi_{n+1} \leq \psi_n + \alpha_n(\psi_n - \psi_{n-1}) + \delta_n$ *for all* $n \geq 1$, $\sum_{n=1}^{\infty} \delta_n < +\infty$ *and there exists a real number* α *with* $0 \leq \alpha_n \leq \alpha < 1$ *for all* $n \geq 1$. *Then the followings hold:*
(i) $\Sigma_{n\geq 1}[\psi_n - \psi_{n-1}]_+ < +\infty$, *where* $[t]_+ = \max\{t, 0\}$*;*
(ii) There exists $\psi^* \in [0,+\infty)$ *such that* $\lim_{n\to+\infty} \psi_n = \psi^*$.

Lemma 2.2. [26] *Let* $\boldsymbol{X}$ *be a Banach space satisfying Opial's condition and let* $\{x_n\}$ *be a sequence in* $\boldsymbol{X}$. *Let* $u, v \in \boldsymbol{X}$ *be such that*

$$\lim_{n\to\infty} \|x_n - u\| \quad and \quad \lim_{n\to\infty} \|x_n - v\| \quad exist.$$

If $\{x_{n_k}\}$ *and* $\{x_{m_k}\}$ *are subsequences of* $\{x_n\}$ *which converge weakly to* u *and* v, *respectively, then* $u = v$.

Definition 2.3. Let $G = (V(G), E(G))$ be a directed graph and (u, v) be a directed edge from vertex u to vertex v. A graph G is called transitive if for any $u, v, z \in V(G)$ such that (u, v) and (v, z) are in $E(G)$, then $(u, z) \in E(G)$.

Definition 2.4. [28] Let $u_0 \in V(G)$ and A subset of $V(G)$. We say that

(i) A is dominated by u_0 if $(u_0, u) \in E(G)$ for all $u \in A$.
(ii) A dominates u_0 if for each $u \in A$, $(u, u_0) \in E(G)$.

Definition 2.5. Let $G = (V(G), E(G))$ be a directed graph. The set of edges $E(G)$ is said to be convex if $(u_i, v_i) \in E(G)$ for all $i = 1, 2, ..., N$ and $\alpha_i \in (0, 1)$ such that $\sum_{i=1}^{N} \alpha_i = 1$, then $(\sum_{i=1}^{N} \alpha_i u_i, \sum_{i=1}^{N} \alpha_i v_i) \in E(G)$.

Lemma 2.6. [24] *Let* C *be a nonempty, closed and convex subset of a Hilbert space* $\boldsymbol{H}$ *and* $G = (V(G), E(G))$ *a directed graph such that* $V(G) = C$. *Let* $T : C \to C$ *be a* $G-$*nonexpansive mapping and* $\{u_n\}$ *be a sequence in* C *such that* $u_n \rightharpoonup u$ *for some* $u \in C$. *If there exists a subsequence* $\{u_{n_k}\}$ *of* $\{u_n\}$ *such that* $(u_{n_k}, u) \in E(G)$ *for all* $k \in \mathbb{N}$ *and* $\{u_n - Tu_n\} \to v$ *for some* $v \in \boldsymbol{H}$. *Then* $(I - T)u = v$.

3. Main results

In this section, we prove the following weak convergence theorem to find a common fixed point of a finite family of G-nonexpansive mappings in Hilbert spaces endowed with a graph.

Theorem 3.1. *Let* C *be a nonempty closed and convex subset of a real Hilbert space* $\boldsymbol{H}$ *and let* $G = (V(G), E(G))$ *be a transitive directed graph such that* $V(G) = C$ *and* $E(G)$ *is convex. Let* $T_i : C \longrightarrow C$ *be a family of* G-*nonexpansive mappings for all* $i = 1, 2, ..., N$ *such that* $F = \bigcap_{i=1}^{N} F(T_i) \neq \emptyset$. *Let* $\{x_n\}$, $\{w_n\}$ *generated by* $x_0, x_1 \in C$ *and*

$$
\begin{cases}
w_n = x_n + \theta_n(x_n - x_{n-1}),\\
y_n^i = (1-\beta_n^i)w_n + \beta_n^i T_i w_n,\\
z_n^i = (1-\alpha_n^i)T_i w_n + \alpha_n^i T_i y_n^i,\\
x_{n+1} = \arg\max\{\|z_n^i - w_n\| : i = 1,2,...,N\},
\end{cases}
\tag{3.1}
$$

where $\{\theta_n\} \subset [0,\theta]$ *for each* $\theta \in (0,1]$ *and* $\{\alpha_n^i\}$ *and* $\{\beta_n^i\}$ *are sequences in* $[0,1]$. *Assume that the following conditions are satisfied:*

(i) $\sum_{n=1}^{\infty} \theta_n \|x_n - x_{n-1}\| < \infty$*;*
(ii) $\{w_n\}$ *is dominated by* t *and* $\{w_n\}$ *dominates* t *for all* $t \in F$*, and if there exists a subsequence* $\{w_{n_k}\}$ *of* $\{w_n\}$ *such that* $\{w_{n_k}\} \rightharpoonup u \in C$*, then* $(\{w_{n_k}\}, u) \in E(G)$*;*
(iii) $\liminf_{n\to\infty} \alpha_n^i > 0$*;*
(iv) $0 < \liminf_{n\to\infty} \beta_n^i \le \limsup_{n\to\infty} \beta_n^i < 1$.

Then the sequence $\{x_n\}$ *converges weakly to an element in* F.

Proof. Let $t \in F$. Since $\{w_n\}$ dominates t and T_i is edge-preserving, we get $(T_i w_n, t) \in E(G)$ for all $i = 1,2,...,N$. Implying thereby $(y_n^i, t) = \left((1-\beta_n^i)w_n + \beta_n^i T_i w_n, t\right) \in E(G)$ by $E(G)$ is convex. For all $i = 1,2,...,N$, we get

$$
\begin{aligned}
\left\|z_n^i - t\right\| &= \left\|(1-\alpha_n^i)(T_i w_n - t) + \alpha_n^i(T_i y_n^i - t)\right\|\\
&\le (1-\alpha_n^i)\|T_i w_n - t\| + \alpha_n^i \left\|T_i y_n^i - t\right\|\\
&\le (1-\alpha_n^i)\|w_n - t\| + \alpha_n^i \left\|y_n^i - t\right\|\\
&= (1-\alpha_n^i)\|w_n - t\| + \alpha_n^i \left\|(1-\beta_n^i)(w_n - t) + \beta_n^i(T_i w_n - t)\right\|\\
&\le (1-\alpha_n^i)\|w_n - t\| + \alpha_n^i \left\{(1-\beta_n^i)\|w_n - t\| + \beta_n^i \|T_i w_n - t\|\right\}\\
&\le \|w_n - t\|\\
&\le \|x_n - t\| + \theta_n\|x_n - x_{n-1}\|.
\end{aligned}
$$

This implies that $\|x_{n+1} - t\| \le \|x_n - t\| + \theta_n\|x_n - x_{n-1}\|$. From Lemma 2.1 and the assumption (i), we obtain $\lim_{n\to\infty}\|x_n - t\|$ exists, in particular, $\{x_n\}$ is bounded and also $\{y_n^i\}$ and $\{z_n^i\}$. By the properties in a real Hilbert space $\boldsymbol{H}$, we have

$$
\begin{aligned}
\|z_n^i - t\|^2 &\le (1-\alpha_n^i)\|T_i w_n - t\|^2 + \alpha_n^i\|T_i y_n^i - t\|^2\\
&\le (1-\alpha_n^i)\|w_n - t\|^2 + \alpha_n^i\|y_n^i - t\|^2\\
&\le (1-\alpha_n^i)\|w_n - t\|^2\\
&\quad + \alpha_n^i((1-\beta_n^i)\|w_n - t\|^2 + \beta_n^i\|T_i w_n - t\|^2 - (1-\beta_n^i)\beta_n^i\|T_i w_n - w_n\|^2)\\
&\le \|w_n - t\|^2 - \alpha_n^i(1-\beta_n^i)\beta_n^i\|T_i w_n - w_n\|^2\\
&\le \|x_n - t\|^2 + 2\theta_n\langle x_n - x_{n-1}, w_n - t\rangle - \alpha_n^i(1-\beta_n^i)\beta_n^i\|T_i w_n - w_n\|^2.
\end{aligned}
\tag{3.2}
$$

This implies that there exist $i_n \in \{1,2,...,N\}$ such that

$$
\alpha_n^{i_n}(1-\beta_n^{i_n})\beta_n^{i_n}\|T_{i_n} w_n - w_n\|^2 \le \|x_n - t\|^2 - \|x_{n+1} - t\|^2 + 2\theta_n\langle x_n - x_{n-1}, w_n - t\rangle. \tag{3.3}
$$

By the assumptions (i), (iii) and (iv), from (3.3) and $\lim_{n\to\infty}\|x_n - t\|$ exist, we have

$$\lim_{n\to\infty}\|T_{i_n}w_n - w_n\| = 0. \tag{3.4}$$

By the definition of our algorithm and the assumption (iv), we have

$$\|y_n^{i_n} - w_n\| = \beta_n^{i_n}\|T_{i_n}w_n - w_n\| \to 0 \tag{3.5}$$

as $n \to \infty$. Since $(w_n, t), (t, y^{i_n}) \in E(G)$, so $(w_n, y^{i_n}) \in E(G)$. It follows from (3.5) that

$$\|x_{n+1} - T_{i_n}w_n\| = \alpha_n^{i_n}\|T_{i_n}y_n^{i_n} - T_{i_n}w_n\| \le \alpha_n^{i_n}\|y_n^{i_n} - w_n\| \to 0 \tag{3.6}$$

as $n \to \infty$. From (3.4) and (3.6), we have

$$\lim_{n\to\infty}\|x_{n+1} - w_n\| = 0. \tag{3.7}$$

This implies that

$$\|z_n^i - w_n\| \le \|x_{n+1} - w_n\| \to 0 \tag{3.8}$$

as $n \to \infty$ for all $i = 1, 2, ..., N$. From (3.2), we have

$$\alpha_n^i(1 - \beta_n^i)\beta_n^i\|T_iw_n - w_n\|^2 \le \|w_n - t\|^2 - \|z_n^i - t\|^2. \tag{3.9}$$

By our assumptions (iii) and (iv), it follows from (3.8) and (3.9) that

$$\lim_{n\to\infty}\|T_iw_n - w_n\| = 0, \tag{3.10}$$

for all $i = 1, 2, ..., N$.

Since $\{w_n\}$ is bounded and $\boldsymbol{H}$ is reflexive, $\omega_w(w_n) = \{x \in \boldsymbol{H} : w_{n_k} \rightharpoonup p, \{w_{n_k}\} \subset \{w_n\}\}$ is nonempty. Let $p \in \omega_w(w_n)$ be an arbitrary element. Then there exists a subsequence $\{w_{n_k}\} \subset \{w_n\}$ converging weakly to p. Let $q \in \omega_w(w_n)$ and $\{w_{n_m}\} \subset \{w_n\}$ be such that $w_{n_m} \rightharpoonup q$. From Lemma 2.6 and (3.10), we have $p, q \in F$. Applying Lemma 2.2, we obtain $p = q$. □

We know that if T is nonexpansive, that T is G-nonexpansive. From direct consequences of Theorem 3.1, we have the following corollary:

Corollary 3.2. *Let C be a nonempty closed and convex subset of a real Hilbert space $\boldsymbol{H}$, and let $T_i : C \longrightarrow C$ be a family of nonexpansive mappings for all $i = 1, 2, ..., N$ such that $F = \bigcap_{i=1}^{N} F(T_i) \neq \emptyset$. Let $\{x_n\}$, $\{w_n\}$ generated by $x_0, x_1 \in C$ and*

$$\begin{cases} w_n = x_n + \theta_n(x_n - x_{n-1}), \\ y_n^i = (1 - \beta_n^i)w_n + \beta_n^i T_i w_n, \\ z_n^i = (1 - \alpha_n^i)T_i w_n + \alpha_n^i T_i y_n^i, \\ x_{n+1} = \arg\max\{\|z_n^i - w_n\| : i = 1, 2, ..., N\}, \end{cases} \tag{3.11}$$

where $\{\theta_n\} \subset [0, \theta]$ for each $\theta \in (0, 1]$ and $\{\alpha_n^i\}$ and $\{\beta_n^i\}$ are sequences in $[0, 1]$. Assume that the following conditions are satisfied:

(i) $\sum_{n=1}^{\infty}\theta_n\|x_n - x_{n-1}\| < \infty$*;*
(ii) $\liminf_{n\to\infty} \alpha_n^i > 0$*;*
(iii) $0 < \liminf_{n\to\infty} \beta_n^i \le \limsup_{n\to\infty} \beta_n^i < 1$.

Then the sequence $\{x_n\}$ converges weakly to an element in F.

4. Application to signal recovery

A signal recovery problem can be modeled as the following underdetermined linear equation system:

$$v = Au + \epsilon, \tag{4.1}$$

where $u \in \mathbb{R}^{\bar{N}}$ is an original signal, $v \in \mathbb{R}^M$ is the observed signal which is squashed by the filter matrix $A : \mathbb{R}^{\bar{N}} \to \mathbb{R}^M$ and noisy ϵ. It is well known that the problem (4.1) can be solved by the LASSO problem:

$$\min_{u \in \mathbb{R}^{\bar{N}}} \frac{1}{2}\|v - Au\|_2^2 + \lambda\|u\|_1, \tag{4.2}$$

where $\lambda > 0$. As a result, various techniques and iterative schemes have been developed over the years to solve the Lasso problem, see [18, 19, 25]. In this case, we set $Tu = \text{prox}_{\lambda g}(u - \lambda\nabla f(u))$, where $f(u) = \frac{1}{2}\|v - Au\|_2^2$ and $g(u) = \lambda\|u\|_1$. It is known that T is a nonexpansive mapping when $\lambda \in (0, 2/L)$ and L is the Lipschitz constant of ∇f.

The goal of this paper is to remove noise without knowing the type of filter and noise. Thus, we are interested in the following common problems which are introduced by Suantai et al. [27]:

$$\begin{aligned} \min_{u \in \mathbb{R}^{\bar{N}}} \frac{1}{2}\|A_1 u - v\|_2^2 &\quad + \quad \lambda_1\|u\|_1, \\ \min_{u \in \mathbb{R}^{\bar{N}}} \frac{1}{2}\|A_2 u - v\|_2^2 &\quad + \quad \lambda_2\|u\|_1, \\ &\quad \vdots \\ \min_{u \in \mathbb{R}^{\bar{N}}} \frac{1}{2}\|A_N u - v\|_2^2 &\quad + \quad \lambda_N\|u\|_1, \end{aligned} \tag{4.3}$$

where u is an original signal, A_i is a bounded linear operator and v_i is an observed signal with noisy for all $i = 1, 2, ..., N$. We can apply our proposed algorithm (3.1) to solve the problem (4.3) by setting $T_i u = \text{prox}_{\lambda_i g_i}(u - \lambda_i \nabla f_i(u))$.

For all experiments in this section, the size of signal is selected to be $\bar{N} = 1024$ and $M = 512$, where the original signal x is generated by the uniform distribution in $[-2, 2]$ with m nonzero elements. Suppose that

$$\theta_n = \begin{cases} \min\left\{\frac{\bar{\theta}_n}{\|x_n - x_{n-1}\|_2}, 0.3\right\} & \text{if } x_n \neq x_{n-1}, \\ 0.3 & \text{otherwise} \end{cases}$$

for all $n \in \mathbb{N}$. In the first part, we solve the problem (4.2) by considering the different components within algorithm (3.1): λ, $\bar{\theta}_n$, β_n^1 and α_n^1. Let A be the Gaussian matrix generated by commend *randn*$(M, \bar{N})$, the observation b be generated by white Gaussian noise with signal-to-noise ratio SNR=40 and $m = 25$. Given that the initial points x_0, x_1 are generated by commend *randn*$(\bar{N}, 1)$. We use the mean-squared error to measure the restoration accuracy defined as follows: $MSE_n = \frac{1}{1024}\|x_n - x\|_2^2 < 10^{-5}$. To find suitable parameters for the next numerical experiments, we present numerical results through Tables 1–4 with different parameters $\bar{\theta}_n$, λ, β_n^1 and α_n^1, respectively.

Case 1. We compare the performance of the algorithm with different parameters $\bar{\theta}_n$ by setting $\lambda = \frac{1}{\|A\|_2^2}, \beta_n^1 = 0.5$ and $\alpha_n^1 = \frac{n}{5(n+1)}$ for all $n \in \mathbb{N}$. Then the results are presented in Table 1.

Table 1. Numerical results of $\bar{\theta}_n$.

$\bar{\theta}_n$	0	$\frac{1}{(n+1)^{1.1}}$	$\frac{1}{(n+1)^2}$	$\frac{100}{(n+1)^2}$	$\frac{1}{(n+100)^2}$
No. of Iter.	3237	2293	2289	3286	2278
Elapsed Time (s)	2.5272	1.5865	1.5386	2.1956	1.5113

Case 2. We compare the performance of the algorithm with different parameters λ by setting $\bar{\theta}_n = \frac{1}{(n+100)^2}$ and select α_n^1 and β_n^1 are the same as in Case 1. Then the results are presented in Table 2.

Table 2. Numerical results of λ.

λ	$\frac{1}{2\|A\|_2^2}$	$\frac{3}{2\|A\|_2^2}$	$\frac{8}{5\|A\|_2^2}$	$\frac{17}{10\|A\|_2^2}$	$\frac{18}{10\|A\|_2^2}$
No. of Iter.	4709	1571	1473	1387	1309
Elapsed Time (s)	3.2404	1.0867	1.0199	0.9493	0.8978

Case 3. We compare the performance of the algorithm with different parameters β_n^1 by setting $\lambda = \frac{18}{10\|A\|_2^2}$, $\bar{\theta}_n = \frac{1}{(n+100)^2}$ and select α_n^1 is the same as in Case 1. Then the results are presented in Table 3.

Table 3. Numerical results of β_n^1.

β_n^1	0.7	0.8	0.9	0.95	0.99
No. of Iter.	1282	1259	1238	1228	1220
Elapsed Time (s)	1.4545	0.9254	0.8734	0.8860	0.8718

Case 4. We compare the performance of the algorithm with different parameters α_n^1 by setting $\lambda = \frac{18}{10\|A\|_2^2}$, $\bar{\theta}_n = \frac{1}{(n+100)^2}$ and $\beta_n^1 = 0.99$. Then the results are presented in Table 4.

Table 4. Numerical results of α_n^1.

α_n^1	$\frac{n}{10(n+1)}$	$\frac{n}{4(n+1)}$	$\frac{n}{2(n+1)}$	$\frac{n}{n+1}$	$\frac{n}{n+100}$
No. of Iter.	1358	1197	1000	753	863
Elapsed Time (s)	0.9990	1.0939	1.2328	0.5437	0.6133

We noticed that in all the above 4 cases, selecting $\alpha_n^1 = \frac{n}{n+1}$ for all $n \in \mathbb{N}$ and setting $\lambda, \bar{\theta}_n$ and β_n^1 as in Case 4, yield the best results.

In the next experiment, we would like to compare the performance of the parallel monotone hybrid algorithm (1.1), inertial parallel monotone hybrid algorithm (1.2) and algorithm (3.1) for solving the problem (4.3) with three filters, that is $N = 3$. The original signal is generated by the uniform distribution in the interval $[-2, 2]$ with m nonzero element. Let A_i be the Gaussian matrix generated by commend $randn(M, \bar{N})$, the observation b_i be generated by white Gaussian noise with signal-to-noise ratio SNR=40, we choose $\lambda_i = \frac{18}{10\|A_i\|_2^2}$, $\beta_n^i = 0.99$ and $\alpha_n^i = \frac{n}{n+1}$ for all $i = 1, 2, 3$, $n \in \mathbb{N}$ and $\bar{\theta}_n = \frac{1}{(n+100)^2}$ for our algorithm (3.1). Choosing

$$\alpha_n^i = \begin{cases} \frac{10}{n+10}, & if\ 1 \leq n < K, \\ \frac{10}{K+10}, & otherwise, \end{cases}$$

for all $i = 1, 2, 3$, $n \in \mathbb{N}$ where K is the number of iterations that we want to stop for the parallel monotone hybrid algorithm (1.1) and $\alpha_n^i = \frac{n}{n+1}$ for all $i = 1, 2, 3$, $n \in \mathbb{N}$ and $\bar{\theta}_n = \frac{1}{(n+100)^2}$ for the inertial parallel monotone hybrid algorithm (1.2). We use $MSE_n < 10^{-5}$. Further, we select x_0 and x_1 are the same as in the first part. The results are presented in Table 5.

Table 5. Numerical comparison of three algorithms.

Algorithms		m Nonzero Elements		
		$m = 50$	$m = 100$	$m = 150$
Parallel monotone hybrid	Elapsed Time (s)	0.3687	0.4073	1.6993
	No. of Iter.	290	317	357
Inertial parallel monotone hybrid	Elapsed Time (s)	0.3297	0.3966	0.9045
	No. of Iter.	260	286	324
Our	Elapsed Time (s)	0.1545	0.1721	0.2365
	No. of Iter.	65	72	89

In the next comparison, we will show the performance of our algorithm comparing with DIO algorithm [20] when $N = 3$. The original signal is generated by the uniform distribution in the interval $[-2, 2]$ with m nonzero element. We suppose A_i, b_i, λ_i, $\bar{\theta}_n$, β_n^i, α_n^i, x_0 and x_1 are the same as in the second part for our algorithm. For DIO algorithm, we choose $x_{1,1} = x_{2,1} = x_{3,1} = x_1$, $a_{i1,n} = a_{i2,n} = \frac{n}{4n+1}$, $a_{i3,n} = (1 - a_{i1,n} - a_{i2,n})$ and $\alpha_{i,n} = 0.3$ for all $i = 1, 2, 3$ and all $n \in \mathbb{N}$. We use $MSE_n < 10^{-5}$. The results are presented in Table 6.

Table 6. Numerical comparison of our algorithm and DIO algorithm.

Algorithms		m Nonzero Elements		
		$m = 50$	$m = 100$	$m = 150$
DIO	Elapsed Time (s)	0.4371	0.4862	0.5984
	No. of Iter.	487	550	604
Our	Elapsed Time (s)	0.1268	0.1295	0.1986
	No. of Iter.	65	74	89

Table 5 shows the comparison of the number of iterations and the time elapsed with $m = 50, 100, 150$ nonzero elements for the three algorithms: Parallel monotone hybrid algorithm, Inertial parallel monotone hybrid algorithm, and our algorithm. For comparison of our algorithm and the DIO are showed in Table 6. In case $m = 150$, the original signal and the measurement of Tables 5 and 6 can be seen in Figures 1 and 4, respectively. The results of the comparison of the three algorithms can be seen in Figures 2 and 3, and the results of DIO algorithm can be seen in Figures 5 and 6. Based on the above results, we can see that our proposed algorithm is less time-consuming and requires fewer iterations than the other three algorithms. We note that the numerical results of the DIO algorithm have been shown for the best of the sequences $\{x_{1,n}\}$, $\{x_{2,n}\}$, $\{x_{3,n}\}$.

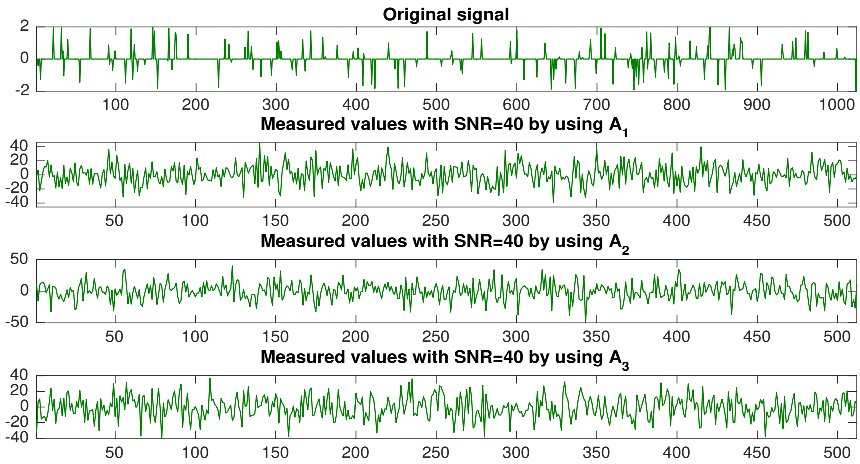

Figure 1. The original signal and the measurement in case $m = 150$ of Table 5.

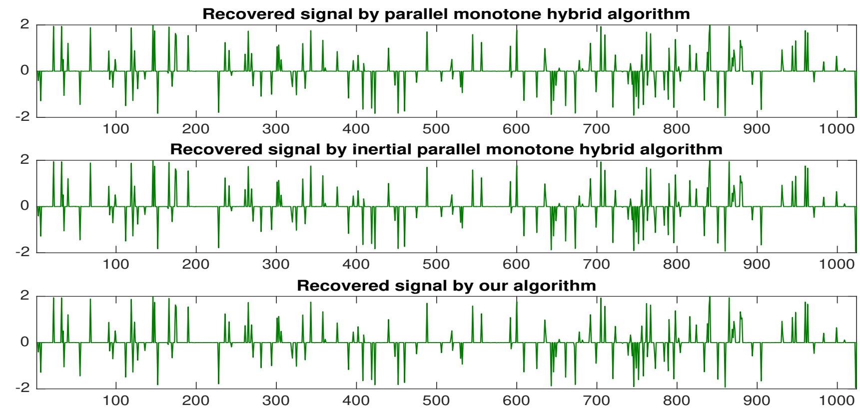

Figure 2. The reconstructed signals by three algorithms in case $m = 150$ of Table 5.

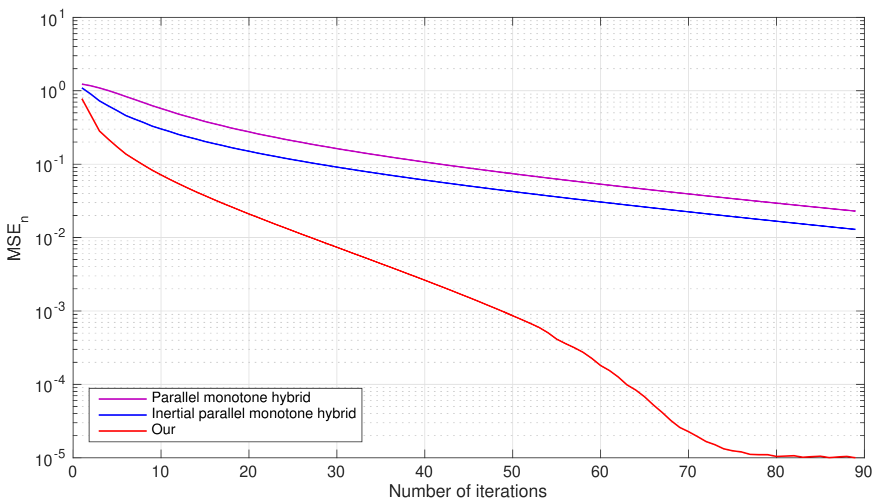

Figure 3. Mean-squared error versus number of iterations in case $m = 150$ of Table 5.

Figure 4. The original signal and the measurement in case $m = 150$ of Table 6.

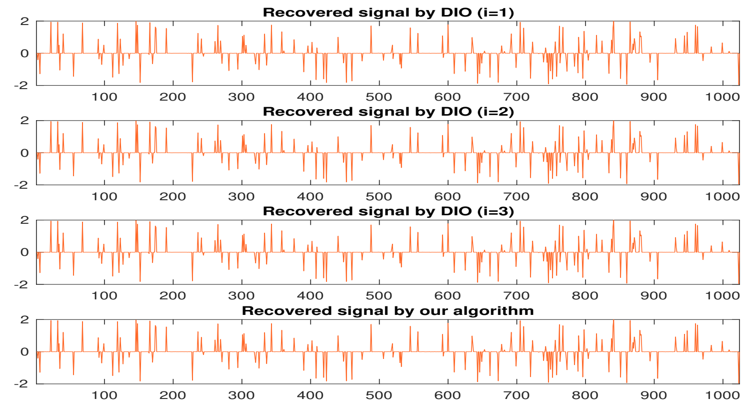

Figure 5. The reconstructed signals by three algorithms in case $m = 150$ of Table 6.

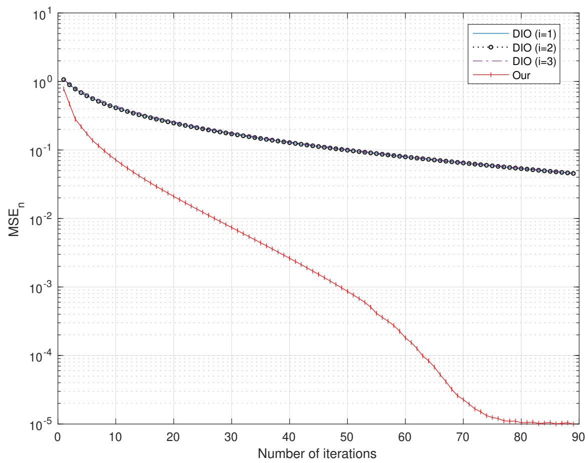

Figure 6. Mean-squared error versus number of iterations in case $m = 150$ of Table 6.

The final experiment considers algorithm (3.1) for solving (4.3) with multiple inputs A_i. The original signal is generated by the uniform distribution in the interval $[-2, 2]$ with m nonzero element. We suppose A_i, b_i, λ_i, $\bar{\theta}_n$, β_n^i, α_n^i, x_0 and x_1 are the same as in the second part. We use $MSE_n < 5 \times 10^{-5}$. The results are following presented in Table 7.

Table 7. Numerical results of our algorithm.

Inputting		m Nonzero Elements			
		$m = 25$	$m = 50$	$m = 75$	$m = 100$
A_1	Elapsed Time (s)	0.6693	0.6887	1.0002	1.1109
	No. of Iter.	776	871	1057	1276
A_2	Elapsed Time (s)	0.5325	0.6218	1.2367	1.0217
	No. of Iter.	753	831	1032	1246
A_3	Elapsed Time (s)	0.5636	0.6798	0.7639	1.0629
	No. of Iter.	751	863	1052	1338
A_1, A_2	Elapsed Time (s)	0.3752	0.4090	0.4521	0.4320
	No. of Iter.	222	216	259	248
A_1, A_3	Elapsed Time (s)	0.3718	0.4255	0.4889	0.5027
	No. of Iter.	206	240	275	295
A_2, A_3	Elapsed Time (s)	0.4876	0.3809	0.4176	0.4791
	No. of Iter.	220	212	234	243
A_1, A_2, A_3	Elapsed Time (s)	0.1978	0.1707	0.1716	0.1785
	No. of Iter.	62	64	68	68

Table 7 presents the numerical results of the number of iterations and the time elapsed with multiple inputs A_i and $m = 25, 50, 75, 100$ nonzero elements for our algorithm. The original signal and the measurement by using A_1–A_3 of Table 7 are shown in Figure 7. From Figures 8 and 9, it can be observed that incorporating all 3 Gaussian matrices (A_1–A_3) into algorithm (3.1) is more effective with respect to time and number of iterations than involving only one or two of them.

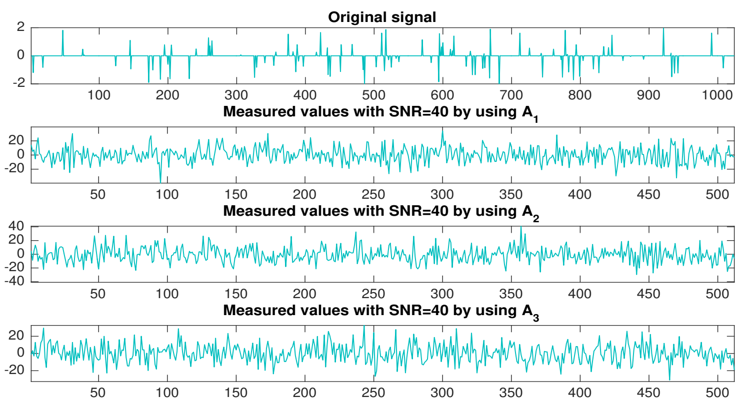

Figure 7. The original signal and the measurement by using A_1–A_3, respectively with m=100.

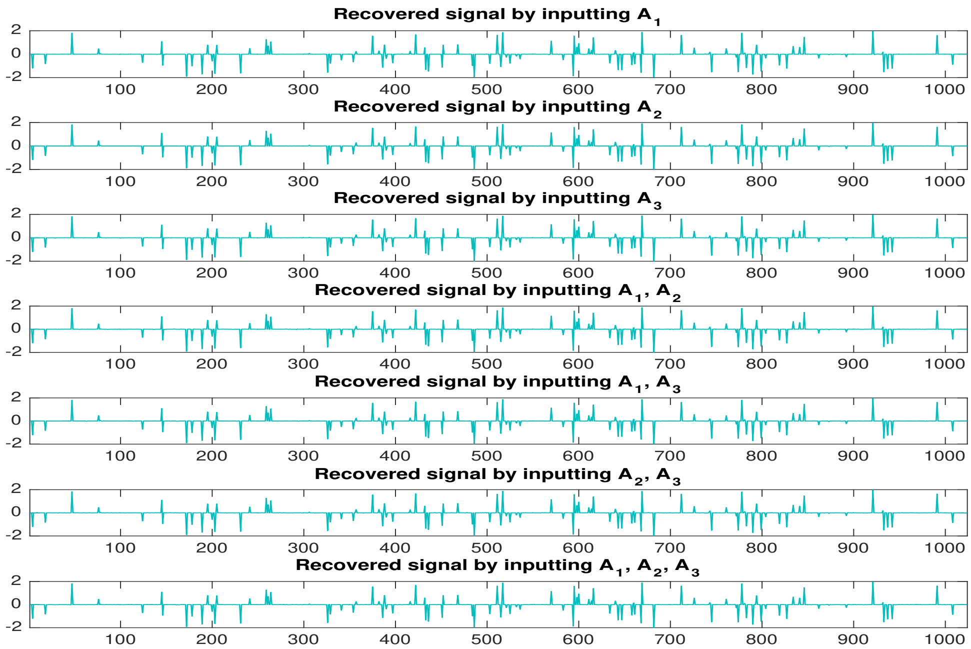

Figure 8. The reconstructed signals by using each input for m=100.

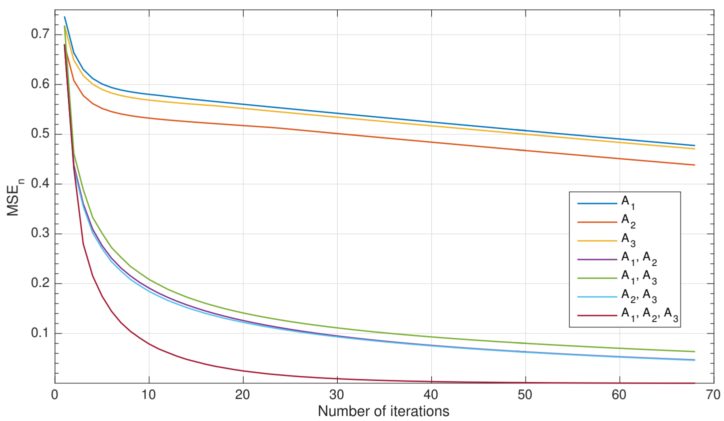

Figure 9. The mean-squared error versus number of iterations for m=100.

5. Conclusions

We introduce a new inertial parallel algorithm to solve the common fixed point problem for a finite family of G-nonexpansive mappings in a Hilbert space with a directed graph. Our primary theorems ensure that this algorithm converges weakly to an element of the problem's solution set under certain conditions. The algorithm is then used to solve the signal recovery problem involving several filters.

Acknowledgments

This research project was supported by the Thailand Science Research and Innovation Fund and the University of Phayao (Grant No. FF64-UoE002).

Conflict of interest

The authors declare that they have no competing interests.

References

1. R. P. Agarwal, D. O'Regan, D. R. Sahu, Iterative construction of fixed points of nearly asymptotically nonexpansive mappings, *J. Nonlinear Convex A.*, **8** (2007), 61–79. doi: 10.1007/s10851-006-9699-4.
2. S. M. A. Aleomraninejad, S. Rezapour, N. Shahzad, Some fixed point results on a metric space with a graph, *Topol. Appl.*, **159** (2012), 659–663. doi: 10.1016/j.topol.2011.10.013.
3. M. R. Alfuraidan, M. A. Khamsi, Fixed points of monotone nonexpansive mappings on a hyperbolic metric space with a graph, *Fixed Point Theory A.*, **2015** (2015), 1–10. doi: 10.1186/s13663-015-0294-5.
4. M. R. Alfuraidan, On monotone Ćirić quasi-contraction mappings with a graph, *Fixed Point Theory A.*, **2015** (2015), 1–11. doi: 10.1186/s13663-015-0341-2.
5. F. Alvarez, H. Attouch, An inertial proximal method for maximal monotone operators via discretization of a nonlinear oscillator with damping, *Set-Valued Anal.*, **9** (2001), 3–11. doi: 10.1023/A:1011253113155.
6. P. K. Anh, D. V. Hieu, Parallel and sequential hybrid methods for a finite family of asymptotically quasi ϕ-nonexpansive mappings, *J. Appl. Math. Comput.*, **48** (2015), 241–263. doi: 10.1007/s12190-014-0801-6.
7. P. K. Anh, D. V. Hieu, Parallel hybrid iterative methods for variational inequalities, equilibrium problems, and common fixed point problems, *Vietnam J. Math.*, **44** (2016), 351–374. doi: 10.1007/s10013-015-0129-z.
8. H. Attouch, J. Peypouquet, P. Redont, A dynamical approach to an inertial forward-backward algorithm for convex minimization, *SIAM J. Optimiz.*, **24** (2014), 232–256. doi: 10.1137/130910294.
9. A. Beck, M. Teboulle, A fast iterative shrinkage-thresholding algorithm for linear inverse problems, *SIAM J. Imaging Sci.*, **2** (2009), 183–202. doi: 10.1137/080716542.
10. P. Cholamjiak, S. Suantai, P. Sunthrayuth, An explicit parallel algorithm for solving variational inclusion problem and fixed point problem in Banach spaces, *Banach J. Math. Anal.*, **14** (2020), 20–40. doi: 10.1007/s43037-019-00030-4.
11. W. Cholamjiak, S. A. Khan, D. Yambangwai, K. R. Kazmi, Strong convergence analysis of common variational inclusion problems involving an inertial parallel monotone hybrid method

for a novel application to image restoration, *RACSAM Rev. R. Acad. A*, **114** (2020), 1–20. doi: 10.1007/s13398-020-00827-1.

12. D. V. Hieu, A parallel hybrid method for equilibrium problems, variational inequalities and nonexpansive mappings in Hilbert space, *J. Korean Math. Soc.*, **52** (2015), 373–388. doi: 10.4134/JKMS.2015.52.2.373.
13. D. V. Hieu, Y. J. Cho, Y. B. Xiao, P. Kumam, Modified extragradient method for pseudomonotone variational inequalities in infinite dimensional Hilbert spaces, *Vietnam J. Math.*, **49** (2021), 1165–1183. doi: 10.1007/s10013-020-00447-7.
14. D. V. Hieu, L. D. Muu, P. K. Anh, Parallel hybrid extragradient methods for pseudomonotone equilibrium problems and nonexpansive mappings, *Numer. Algorithms*, **73** (2016), 197–217. doi: 10.1007/s11075-015-0092-5.
15. D. V. Hieu, Parallel and cyclic hybrid subgradient extragradient methods for variational inequalities, *Afr. Math.*, **28** (2017), 677–692. doi: 10.1007/s13370-016-0473-5.
16. D. V. Hieu, Parallel hybrid methods for generalized equilibrium problems and asymptotically strictly pseudocontractive mappings, *J. Appl. Math. Comput.*, **53** (2017), 531–554. doi: 10.1007/s12190-015-0980-9.
17. J. Jachymski, The contraction principle for mappings on a metric space with a graph, *Proc. Am. Math. Soc.*, **136** (2008), 1359–1373. doi: 10.1090/S0002-9939-07-09110-1.
18. K. Kankam, N. Pholasa, P. Cholamjiak, On convergence and complexity of the modified forward-backward method involving new linesearches for convex minimization, *Math. Method. Appl. Sci.*, **42** (2019), 1352–1362. doi: 10.1002/mma.5420.
19. D. Kitkuan, P. Kumam, J. Martínez-Moreno, K. Sitthithakerngkiet, Inertial viscosity forward-backward splitting algorithm for monotone inclusions and its application to image restoration problems, *Int. J. Comput. Math.*, **97** (2020), 482–497. doi: 10.1080/00207160.2019.1649661.
20. X. Li, G. Feng, Distributed algorithms for computing a common fixed point of a group of nonexpansive operators, *IEEE T. Automat Contr.*, **66** (2020), 2130–2145. doi: 10.1109/TAC.2020.3004773.
21. P. E. Maingé, Regularized and inertial algorithms for common fixed points of nonlinear operators, *J. Math. Anal. Appl.*, **344** (2008), 876–887. doi: 10.1016/j.jmaa.2008.03.028.
22. B. T. Polyak, Some methods of speeding up the convergence of iterative methods, *USSR Comput. Math. Math. Phys.*, **4** (1964), 1–17. doi: 10.1016/0041-5553(64)90137-5.
23. P. Sridarat, R. Suparatulatorn, S. Suantai, Y. J. Cho, Convergence analysis of SP-iteration for G-nonexpansive mappings with directed graphs, *Bull. Malays. Math. Sci. Soc.*, **42** (2019), 2361–2380. doi: 10.1007/s40840-018-0606-0.
24. S. Suantai, M. Donganont, W. Cholamjiak, Hybrid methods for a countable family of G-nonexpansive mappings in Hilbert spaces endowed with graphs, *Mathematics*, **7** (2019), 1–13. doi: 10.3390/math7100936.
25. S. Suantai, K. Kankam, P. Cholamjiak, A novel forward-backward algorithm for solving convex minimization problem in Hilbert spaces, *Mathematics*, **8** (2020), 1–13. doi: 10.3390/math8010042.

26. S. Suantai, Weak and strong convergence criteria of Noor iterations for asymptotically nonexpansive mappings, *J. Math. Anal. Appl.*, **311** (2005), 506–517. doi: 10.1016/j.jmaa.2005.03.002.

27. S. Suantai, K. Kankam, P. Cholamjiak, W. Cholamjiak, A parallel monotone hybrid algorithm for a finite family of G-nonexpansive mappings in Hilbert spaces endowed with a graph applicable in signal recovery, *Comp. Appl. Math.*, **40** (2021), 1–17. doi: 10.1007/s40314-021-01530-6.

28. R. Suparatulatorn, W. Cholamjiak, S. Suantai, A modified S-iteration process for G-nonexpansive mappings in Banach spaces with graphs, *Numer. Algorithms*, **77** (2018), 479–490. doi: 10.1007/s11075-017-0324-y.

29. R. Suparatulatorn, S. Suantai, W. Cholamjiak, Hybrid methods for a finite family of G-nonexpansive mappings in Hilbert spaces endowed with graphs, *AKCE Int. J. Graphs Co.*, **14** (2017), 101–111. doi: 10.1016/j.akcej.2017.01.001.

30. D. V. Thong, D. V. Hieu, Inertial extragradient algorithms for strongly pseudomonotone variational inequalities, *J. Comput. Appl. Math.*, **341** (2018), 80–98. doi: 10.1016/j.cam.2018.03.019.

31. D. V. Thong, D. V. Hieu, Modified subgradient extragradient method for variational inequality problems, *Numer. Algorithms*, **79** (2018), 597–610. doi: 10.1007/s11075-017-0452-4.

32. J. Tiammee, A. Kaewkhao, S. Suantai, On Browder's convergence theorem and Halpern iteration process for G-nonexpansive mappings in Hilbert spaces endowed with graphs, *Fixed Point Theory A.*, **2015** (2015), 1–12. doi: 10.1186/s13663-015-0436-9.

33. O. Tripak, Common fixed points of G-nonexpansive mappings on Banach spaces with a graph, *Fixed Point Theory A.*, **2016** (2016), 1–8. doi: 10.1186/s13663-016-0578-4.

34. L. Y. Zhang, H. Zhao, Y. B. Lv, A modified inertial projection and contraction algorithms for quasivariational inequalities, *Appl. Set-Valued Anal. Optim.*, **1** (2019), 63–76. doi: 10.23952/asvao.1.2019.1.06.

AIMS Press